Comparison of tissue abundance of non-cytochrome P450 drug metabolizing enzymes by quantitative proteomics between humans and laboratory animal species

Abdul Basit[1], Peter W. Fan[2], S. Cyrus Khojasteh[3], Bernard P. Murray[4], Bill J. Smith[4], Scott Heyward[5], and Bhagwat Prasad[1]

[1]Department of Pharmaceutical Sciences, Washington State University, Spokane, WA 99202

[2]Department of Pharmacokinetics, Pharmacodynamics and Drug Metabolism Merck & Co., Inc. 33 Avenue Louis Pasteur Boston, MA 02115

[3]Department of Drug Metabolism and Pharmacokinetics, Genentech Inc., 1 DNA Way, MS 412a, South San Francisco, CA 94080

[4]Drug Metabolism and Pharmacokinetics Department, Gilead Sciences Inc., 324 Lakeside Drive, Foster City CA 94404

[5]BioIVT Inc., Baltimore, MD, 21227

Running title: Protein abundance of non-CYP enzymes across species

Corresponding Author: Bhagwat Prasad, Ph.D.

Address: Department of Pharmaceutical Sciences, Washington State University, 412 E Spokane Falls Blvd. Spokane, WA 99202. Email: bhagwat.prasad@wsu.edu. Phone: 509-358-7739

Number of-

Manuscript pages: 26

Figures: 5

Tables: 2

References: 25

Number of words in the-

Abstract: 248

Introduction: 712

Discussion: 810

Abbreviations:

ABC: Ammonium Bicarbonate

ADME: Absorption, Distribution, Metabolism, and Excretion

AOX: Aldehyde Oxidase

BCA: Bicinconinic Acid

BSA: Bovine Serum Albumin

CCA: Clopidogrel Carboxylic Acid

CES: Carboxylesterase

DME: Drug Metabolizing Enzyme

DTT: Dithieothreitol

HSA: Human Serum Albumin

IAA: Iodoacetamide

Mdr: Multidrug Resistance Protein

MRP: Multidrug Resistance Associated Protein

Non-CYP: Non-Cytochrome P450

OAT: Organic Anion Transporter

PBPK: Physiologically-Based Pharmacokinetic

PD: Pharmacodynamics

P-gp: P-glycoprotein

PK: Pharmacokinetics

SULT: Sulfotransferase

UGT: UDP-glucuronosyltransferase

ABSTRACT

The use of animal pharmacokinetic models as surrogates for humans relies on the assumption that the drug disposition mechanisms are similar between preclinical species and humans. However, significant cross-species differences exist in the tissue distribution and protein abundance of drug metabolizing enzymes (DMEs) and transporters. We quantified non-cytochrome P450 (non-CYP) DMEs across commonly used preclinical species (cynomolgus and rhesus monkeys, beagle dog, Sprague Dawley and Wistar Han rats, and CD1 mouse) and compared these data with previously obtained human data. Aldehyde oxidase (AOX) was abundant in humans and monkeys while poorly expressed in rodents, and not expressed in dogs. Carboxylesterase 1 (CES1) abundance was highest in the liver while CES2 was primarily expressed in the intestine in all species with notable species differences. For example, hepatic CES1 was 3-fold higher in humans than in monkeys, but hepatic CES2 was 3-5-fold higher in monkeys than in humans. Hepatic glucuronosyltransferase 1A2 (UGT1A2) abundance was ~4 fold higher in dog compared to rat, whereas UGT1A3 abundance was 3-5-fold higher in the dog liver than its orthologue in the human and monkey liver. UGT1A6 abundance was 5-6-fold higher in human liver compared to monkey and dog liver. Hepatic sulfotransferase 1B1 (SULT1B1) abundance was 5-7-fold higher in rats compared to the rest of the species. These quantitative non-CYP proteomics data can be used to explain unique toxicological profiles across species and can be integrated into physiologically-based pharmacokinetic (PBPK) models for the mechanistic explanation of pharmacokinetics and tissue distribution of xenobiotics in animal species.

SIGNIFICANCE STATEMENT

We characterized the quantitative differences in non-cytochrome P450 (non-CYP) drug metabolizing enzymes across commonly used preclinical species (cynomolgus and rhesus monkeys, beagle dog, Sprague Dawley and Wistar Han rats, and CD1 mouse) and compared these data with previously obtained human data. Unique differences in non-CYP enzymes across species were observed, which can be used to explain significant pharmacokinetic and toxicokinetic differences between experimental animals and humans.

DMD Fast Forward. Published on December 30, 2021 as DOI: 10.1124/dmd.121.000774
This article has not been copyedited and formatted. The final version may differ from this version.

1. INTRODUCTION

Preclinical models are an integral part of the drug discovery and development process. Despite advanced in vitro models, preclinical pharmacokinetics (PK) and toxicity data conducted in laboratory animal species are the foundation of investigational new drug applications (Barre-Sinoussi and Montagutelli, 2015). Moreover, exploratory tissue distribution studies can only be performed in preclinical species. The commonly used preclinical species in drug testing are mouse (CD1), rat (Sprague Dawley and Wistar Han), dog (beagle), and non-human primates (cynomolgus and rhesus). These preclinical models have several advantages, which include i) they represent complete physiological systems for absorption, distribution, metabolism, and excretion (ADME) processes, ii) both PK and pharmacodynamics (PD) can be studied simultaneously, and ii) less ethical hurdles as compared to clinical studies (Barre-Sinoussi and Montagutelli, 2015). However, animal studies are often associated with limitations of interspecies differences in the processes that govern ADME and PD.

With respect to drug disposition, experimental animals are significantly different from humans. While monkey is genetically the closest species to human, both protein abundance as well as substrate affinity (Km) to enzymes and transporters can be largely different between human and monkey. An antiviral agent, favipiravir, which is converted into the inactive oxidative metabolite mainly by aldehyde oxidase (AOX), shows large interspecies differences in its metabolism with highest metabolic clearance in monkeys followed by humans > mice > rats (Hanioka et al., 2021). The abundance of organic anion transporter 1 (OAT1), organic cation / carnitine transporter 2 (OCTN2), and multidrug resistance associated protein 4 (MRP4) in kidney tissues is ~3-fold higher in monkeys than humans (Basit et al., 2019). The abundance of multidrug resistance protein (Mdr1) or P-glycoprotein (P-gp) is higher in the male versus female kidney in rats, whereas its abundance in the mouse kidney is significantly higher in females than males (Basit et al., 2019). Therefore, it is important that the abundance and activity of enzymes and

transporters are characterized across species. While cross-species data are available on transporters and CYPs (Wang et al., 2015; Basit et al., 2019; Hammer et al., 2021), protein abundance data for non-CYP enzymes are lacking, which is often associated with the uncertainty in predicting human PK and toxicity of investigational drugs. A notable example is the unpredictable nephrotoxicity associated with an insoluble AOX metabolite, 2-quinolinone-SGX523, in humans (Diamond et al., 2010). Insufficient efflux of this metabolite is the likely cause of its accumulation in the human kidney leading to nephrotoxicity that can be explained by differences in the protein abundance as well as the substrate affinity to the transporters in the kidney. Variable rates of hydrolysis of clopidogrel to its inactive but major metabolite, clopidogrel carboxylic acid (CCA) across species highlight the species difference in carboxylesterase 1 (CES1) mediated hydrolysis. In particular, the formation rate of CCA was slowest in rats and fastest in minipig (Wang et al., 2020). This variability in hydrolysis of prodrug across species might complicate the dose extrapolation from one species to another and may lead to either loss of efficacy or higher exposure associated with adverse events (Wang et al., 2020).

The lack of specific probe substrates, inhibitors, and in vitro models to study non-CYP enzymes are other critical challenges. Further, knowledge gap with respect to the extrahepatic abundance of non-CYP enzymes adds additional challenges in predicting their role in drug metabolism and toxicity. Further, non-CYP metabolites formed by CESs and AOX are often associated with secondary metabolism, which can become rate limiting in the elimination of the primary metabolites from tissues. In such cases, it is pertinent to understand the critical rate limiting step(s) (primary metabolism) that affects the drug clearance and tissue exposure. Since the metabolism of drugs often involves sequential processes (e.g., Phase I and Phase II metabolism), species differences in the enzyme abundances can affect metabolite profiles in experimental animals versus humans. For example, irinotecan metabolism to SN-38 by CES2 is rate limiting for hepatic SN-38 exposure whereas UGT1A1 is the rate-limiting step for intestinal

SN-38 exposure (Parvez et al., 2021). Therefore, it is important to characterize the relative abundance of sequential enzyme systems such as CES and UGTs. Considering these challenges, we quantified interspecies differences in protein abundance of AOX, CESs, UDP-glucuronosyltransferases (UGTs), and sulfotransferases (SULTs) as a first step towards better interpretation and scaling of preclinical data to human.

2. EXPERIMENTAL SECTION

2.1 Materials

Methanol, MS-grade acetonitrile, and formic acid were purchased from Fisher Scientific (Fair Lawn, NJ). Acetone was purchased from Sigma-Aldrich (St. Louis, MO). Bicinchoninic acid (BCA) kit for total protein quantification was purchased from Pierce Biotechnology (Rockford, IL). Ammonium bicarbonate (ABC) (98% pure), dithiothreitol (DTT), iodoacetamide (IAA), and trypsin were procured from Thermo Fisher Scientific (Rockford, IL). Human serum albumin (HSA) and bovine serum albumin (BSA) were purchased from Calbiochem (Billerica, MA) and Thermo Fisher Scientific (Rockford, IL), respectively. Synthetic unlabeled peptides with amino acid analysis and stable labeled (heavy) peptides were purchased from New England Peptides (Boston, MA) and Thermo Fisher Scientific (Rockford, IL), respectively.

2.2 Procurement of tissue samples from preclinical species and collection of human data

Unless otherwise stated here, tissue homogenate samples from preclinical species were provided by BioIVT Inc. (Baltimore, MD). Pooled Sprague Dawley rat intestinal S9 (n=200), Wistar Han rat liver S9 (n=240), and rhesus monkey pooled liver S9 (n=6) and intestinal S9 (n=7) fractions were procured from SEKISUI Xenotech (Kansas City, KS). The human data were obtained from our previous study (Basit et al., 2020) for which the demographic

information is provided in Supplementary Table S1. The details of the preclinical samples are provided in Table 1.

2.3 S9 subcellular preparation

S9 fractions were prepared from tissue homogenates as described previously (Prasad et al., 2018). Briefly, the homogenate was centrifuged at 9000 x *g* for 30 min at 4°C. The supernatant (S9 fraction) was transferred to a new 1.5 mL centrifuge tube. Total protein in tissue samples was quantified using the BCA assay kit (Pierce Biotechnology, Rockford, IL) following the vendor protocol. S9 fractions were stored at -80 C prior to LC-MS/MS analysis.

2.4 Surrogate peptide selection strategy

Selection of surrogate peptide(s) is the first critical step in targeted proteomics quantification by LC-MS/MS. A detailed list of criteria for selection of signature peptides is described previously (Bhatt and Prasad, 2018) and presented in Supplementary Figure S1. In brief, an ideal peptide should be unique, sensitive, stable, soluble and LC-MS compatible. Surrogate peptides should be unique to the protein of interest in a particular species, which can be confirmed by MS-homology search such as by using Protein Prospector (http://prospector.ucsf.edu/prospector/mshome.htm). In addition, we selected the surrogate peptides which are orthologous in at least one more species to allow quantification using matrix approach (Basit et al., 2019). However, in cases where orthologous peptides were not available, we selected peptides with only 1-3 amino acid differences and retained terminal amino acids to avoid variability in response (Table S2).

2.5 Sample preparation and LC-MS/MS analysis of targeted peptides

The S9 samples were digested using a previously optimized protocol (Ahire et al., 2021). Briefly, 80 µL of S9 sample (1 mg/mL total protein) was mixed with 30 µL ABC (100 mM), and 20 µL of BSA (0.02 mg/mL) in a 1.5 mL microcentrifuge tube. The proteins were denatured and reduced

with 10 µL 250 mM DTT at 95°C for 10 min with gentle shaking at 300 rpm. The sample was cooled to room temperature for 10 min, and the denatured proteins were alkylated with 10 µL of 500 mM IAA in the dark for 30 min. Ice-cold acetone (1 mL) was added to precipitate proteins followed by vortex mixing and centrifugation at 16,000 × *g* (4°C) for 5 min. The supernatant was removed using vacuum suction. The protein pellet was dried for 10 min at room temperature and washed with 500 µL ice-cold methanol followed by centrifugation at 8000 × *g* (4°C) for 5 min. The supernatant was removed, and the pellet was dried at room temperature for 30 min and resuspended in 60 µL ABC buffer (50 mM, pH 7.8). Finally, the resuspended protein sample was digested by adding 20 µL of trypsin (protein: trypsin ratio, ~ 25:1) and incubated at 37°C for 16 hours. The reaction was quenched by the addition of 20 µL of the peptide internal standard cocktail (prepared in 40% acetonitrile in water containing 0.5% formic acid) and 10 µL 1% formic acid in water. The sample was vortex mixed and centrifuged at 4000 ×*g* for 5 min. The supernatant was collected in an LC-MS vial for analysis.

The samples were analyzed using an M-class Waters UPLC system coupled with Waters Xevo TQ-XS µLC-MS/MS instrument supported by IonKey interphase. The peptides were separated on iKey HSS T3 C18 column (130 A°, 1.8 µm, 150 µm x 150 mm) and nano Ease Symmetry C18 trap column (300 µm x 50 mm) (Waters, Milford, MA). The optimized µLC-MS/MS acquisition parameters are provided in Table S3.

2.6 Data analysis

The LC-MS/MS data were analyzed using Skyline 19.1 (University of Washington, Seattle, WA). Briefly, the peptide peaks were identified by matching the retention time with the heavy internal standards and alignment of the selected precursor ion to the respective product ion fragments. A previously optimized robust data analysis approach was used (Wang et al., 2021), which considers the internal standard protein (BSA), heavy internal standard peptide, and previously characterized pooled sample. The absolute protein abundance (pmol/mg protein) was

performed by using a previously characterized pooled sample as the calibrator (Bhatt and Prasad, 2018). Protein abundance data across human tissues were compared using the Kruskal−Wallis test followed by Dunn′s multiple comparison test (across three or more groups) and the Mann−Whitney test (between two groups).

3. RESULTS

In this study, we quantified non-CYP DMEs in human and four commonly used preclinical animal models, i.e., non-human primates (cynomolgus and rhesus monkeys), beagle dogs, Wistar Han and Sprague Dawley rats, and CD-1 mouse across four tissues (liver, intestine, kidney, and heart). These data were compared with our previously generated protein abundance data for human non-CYP DMEs (AOX1, CESs, SULTs and UGTs) (Basit et al., 2020). Wherever the surrogate peptide is conserved in preclinical species and humans, we reported absolute DME abundance data in pmol/mg protein, otherwise, relative abundance data (normalized to total protein) are presented.

3.1 Protein sequence similarity between human and preclinical species and peptide selection for selective quantification

We used UniProt (https://www.uniprot.org/) and NCBI's basic local alignment search tool (BLAST; https://blast.ncbi.nlm.nih.gov/Blast.cgi) to compare the sequence similarity between proteins in human and preclinical species. As shown in Figure 1 and Supplementary Table S4, human and monkey are similar in their protein sequences with greater than 90% sequence similarity except for CES2 in cynomolgus monkey. In dog, rat and mouse, non-CYP enzymes showed 60-80% sequence similarity for AOX, CES and SULTs. Although there are four mammalian isoforms of AOX (AOX1-4), differences exist in the expression of these genes between human and preclinical species. Mouse and rat express four distinct AOX proteins, dog and monkey express two AOX isoforms, whereas humans have only one isoform (Manevski et

al., 2019). Table 2 presents the tissue localization of various AOX isoforms in human, monkey, dog, rat, and mouse. Moreover, as shown in Figure 1, AOX1 is the only hepatic isoform in human, monkey, and rat, although mouse AOX3 is also localized in the liver. Localization of dog AOX proteins is not well characterized. We only quantified AOX1 or its analogous isoforms because humans and most primates contain a single active AOX gene, i.e., AOX1, which has highest sequence similarity with mouse and rat AOX1. Because dogs do not express AOX1, we quantified AOX2 in dogs as it shows >60% sequence similarity with human AOX1.

UGT protein sequences were challenging to compare due to the differences in their nomenclature. For example, UGT2B7 in humans is 89% similar to UGT2B9 or UGT2B18 in cynomolgus monkeys. This poses a challenge in surrogate peptide selection. Therefore, we relied on quantitative proteomics analysis of unique species-specific surrogate peptide(s) for UGT isoforms (Table S2).

3.2 Absolute abundance of non-CYP enzymes in human and non-human primates

Non-human primates share higher similarity in protein sequence (Table 2) and hence it was possible to identify the conserved signature peptides between human and non-human primates (except for UGTs) to quantify and compare the abundance of non-CYP enzymes in human and non-human primates. In general, AOX is highly abundant in the liver compared to other tissues. Hepatic AOX abundance in monkeys was comparable to that in humans (~1.6-fold difference) (Figure 2). In the intestine, AOX is 2.2-fold higher in cynomolgus monkeys compared to in rhesus monkeys, but it is not detectable in the human intestine. Hepatic CES1 abundance was 3-fold higher in humans compared to non-human primates. In contrast, intestinal and kidney abundance in non-human primates is 20-40-fold higher than in humans. Similarly, CES2 abundance is higher in non-human primate intestine as compared to human intestine. In non-

human primates, ~2-fold higher abundance of CES2 was observed in the liver as compared to the intestine. In general, SULT1A1 levels are 3-5-fold higher in both intestine and liver of the non-human primates as compared to corresponding human tissues. Interestingly, SULT1A1 was detected in the kidney of cynomolgus monkey but it was below the limit of quantification in human kidney. Similarly, SULT1B1 and SULT2A1 were also observed in the cynomolgus kidney, whereas it was similar in the liver and the intestine between humans and the non-human primates. Regarding UGTs, the levels of UGT1A1 between the intestine and liver were similar in humans, whereas 2-12 higher intestinal abundance of UGT1A1 was detected in the non-human primates. Hepatic abundance of UGT1A6 was 2-5-fold higher in the non-human primates compared to humans. UGT1A6 was also detected in the monkey intestine and kidney. Hepatic UGT2B4 and UGT2B7 were 6-fold and >3-fold higher in the non-human primates compared to humans. In the intestine and kidney, UGT2B7 levels were comparable between humans and the non-human primates. While UGT2B15 was below the limit of quantification in the human intestine, the non-human primates showed comparable levels of UGT2B15 in the liver and the intestine.

3.3 Hepatic abundance of non-CYP enzymes across species

The majority of non-CYP enzymes were predominantly detected in the liver across all the species (Figure 3). AOX1 is not expressed in dogs and poorly expressed in rodents, however its abundance is 3-5-fold higher in rats as compared to mice. Hepatic CES1 is 3-fold higher in humans than monkeys, but CES2 is 3-5-fold higher in non-human primates than in humans. Hepatic CES2 abundance is 3-10-fold lower in rodents than in humans and monkeys. SULT1A1 abundance in the liver is 4,7,5 and 3-fold higher in the non-human primates, dogs, and rats than in humans, whereas it was 2-fold lower in mice. SULT1B1 abundance is comparable in humans and the non-human primate livers, whereas it is 5-7-fold higher in rats compared to the rest of the species. Hepatic UGT1A2 expression is ~4 fold higher in dogs compared to rats. UGT1A3

abundance is 3-5-fold higher in dog liver than in human and monkey livers. UGT1A6 abundance in the liver is 5-6-fold higher in humans compared to monkeys and dogs.

3.4 Relative extrahepatic to hepatic abundance on non-CYP enzymes across species

AOX is predominantly detected in the liver in all the species, except human and monkey (kidney, intestine) (Figure 4). CES1 expression is higher in the liver, whereas CES2 is predominant in the intestine in all the tested species. UGT1A1, 1A2, 1A3, 1A7, 2B17 and 2B34 were highly expressed in the intestine, whereas UGT1A6, 2B4, 2B7, 2B9, 2B15 and 2B35 were predominantly detected in the liver. SULT1B1, 1E1 and 1A3 expression was higher in the intestine than in the liver. The ratio of enzyme abundance between tissues showed high interspecies variability. The intestine to liver ratio of CES2 abundance was 4 (human), 1 (cynomolgus), 1 (rhesus), 15 (dog), and 20 (rat). While SULT1A1 intestine to liver ratio was similar across humans, monkeys and dogs, it was uniquely expressed in dog kidney (1.5-fold higher than liver). The intestine to liver ratio of SULT1B1 was 8 (human), 5 (cynomolgus), 2 (rhesus monkey), and 35 (dog). The intestine to liver ratio of SULT2A1 and 1E1 showed a similar pattern with a 2- to 4-fold higher ratio in monkeys as compared to humans. Although the intestine to liver ratio for UGT1A1 in humans was 1, the ratio was higher in preclinical species, i.e., 14 (cynomolgus and rhesus monkey), 2.5 (rat), and 1.2 (mouse).

4. DISCUSSION

Animal to human scaling of PK and toxicity data is important for the safety of healthy volunteers or patients as well as to address the high attrition rate in clinical development. However, there are several examples where interspecies differences in drug disposition partly contributed to the discontinuation of clinical candidates (Semino-Mora et al., 1997; Attarwala, 2010). Such

incidences are common if an investigational drug is an AOX substrate. For example, both SGX523 and JNJ-38877605 (Lolkema et al., 2015) were responsible for nephrotoxicity due to the formation of insoluble metabolites mediated by AOX in human kidney and ultimately leading to discontinuation as a clinical candidate. Capmatinib, a highly selective and potent MET (tyrosine kinase receptor) inhibitor also failed due to high interspecies differences in its AOX mediated metabolism and toxicity (Lolkema et al., 2015; Glaenzel et al., 2020). Considering the implications of interspecies differences in drug development, here we provided a quantitative comparison of non-CYP enzymes in humans versus the non-human primates (cynomolgus and rhesus), dog, rat, and mouse. Our results showed large differences both in the cross-species abundance within one organ as well as the relative localization of these enzymes across different tissues.

Our data correlate with interspecies differences in the PK of drugs and may potentially explain drug toxicity. For example, as discussed above, SGX-523 showed renal toxicity in humans despite toxicology experiments performed in rodents and dogs because it is metabolized by AOX to 2-quinolinone-SGX-523 that is accumulated in the human kidney. The high expression of AOX in human and non-human primate compared to rodents and dogs as shown in this study is the likely reason for the toxic levels of the metabolite (Diao and Huestis, 2019). Similarly, a novel EGFR inhibitor, BIBX1382 failed in drug development because of poor oral bioavailability associated with its extensive AOX mediated metabolism in humans as compared to rodents (Uehara et al., 2021). Intestinal toxicity of irinotecan can also be explained by the tissue proteomics data presented here. Irinotecan is converted to active metabolite SN-38 via CES2 and then subsequently glucuronidated by UGT1A1 (Parvez et al., 2021) and both CES2 and UGT1A1 abundance play important roles in the intestinal toxicity. Our data suggest 3.5-fold higher abundance of CES2 in the intestine as compared to the liver lead to the high local concentration of SN38 in the human intestine (Parvez et al., 2021). Since CES2 and UGT

abundances are significantly different across species and organs, the differences in tissue-specific metabolism in human versus preclinical species may be associated with unexpected tissue metabolite profile and toxicity in humans. For example, the ratio of CES2 abundance between intestine to liver in rats is higher than in humans suggesting that irinotecan to SN38 conversion in relation to liver is faster in rats as compared to humans (Figure 4). Similarly, the prodrugs that are hydrolyzed in the intestine by CES enzymes such as dabigatran etexilate, olmesartan, methylphenidate, and temocapril (Di, 2019) would experience variable hydrolysis between species.

The interspecies difference in the abundance of non-CYP enzymes may not be directly used in scaling animal data to humans due to differences in the substrate affinity (Km) to individual proteins (Zou et al., 2018). We propose a systematic workflow that can be integrated into PBPK modeling for quantitative scaling of non-CYP drug metabolism (Figure 5). Here if the recombinant proteins are available from multiple species the potential isoforms involved in metabolism can be shortlisted, which can then be investigated to estimate Km and V_{max} values across species. Finally, the scaling would require normalization of the in vitro clearance data obtained in animal species with abundance as well as K_m data from different species.

One of the interesting observations of our study was that SULT abundance was higher in the intestine as compared to the liver in rodents which is completely opposite in humans. These findings indicate key physiological differences regarding the need of SULT for the metabolism of endobiotics. Further investigations are needed to understand the evolutionary reason for these findings. UGT abundance data across tissues and across species provide new information, but caution should be taken when using these data in animal to human scaling. For example, UGT2B4 in human is similar to UGT2B19/30 in non-human primate and human UGT2B15 is similar in protein sequence to UGT2B20 and UGT2B31 in rhesus monkey and dog, respectively.

In conclusion, comprehensive quantitative information on non-CYP DMEs across preclinical species including the non-human primates (cynomolgus and rhesus monkey), dog, rat (SD and WH), mouse is presented and compared to the human data. This quantitative information on protein abundance of non-CYP DMEs will be useful in i) extrapolation of drug metabolism data from preclinical species to human ii) prediction of species-specific drug tissue disposition, and iii) integration of protein abundance data with enzyme affinity to mechanistically explain the PK and disposition profile in animal species based on the in vitro studies.

Acknowledgements

The authors would like to thank Mr. Matthew Karasu, WSU, Spokane, WA and Dr. Mike Zientek (Takeda California, San Diego, CA) for the technical support in the sample analysis and insightful suggestions on the manuscript, respectively.

Authorship Contributions

Participated in research design: A.B., B.P., P.W.F, S.C.K., B.P.M, B.J.S., S.H.

Conducted experiments: A.B.

Contributed new reagents or analytic tools: S.H.

Performed data analysis: A.B., B.P.

Wrote or contributed to the writing of the manuscript: A.B., B.P., P.W.F, S.C.K., B.P.M, B.J.S.

References

Ahire DS, Basit A, Karasu M, and Prasad B (2021) Ultrasensitive Quantification of Drug-metabolizing Enzymes and Transporters in Small Sample Volume by Microflow LC-MS/MS. *J Pharm Sci* **110:**2833-2840.

Attarwala H (2010) TGN1412: From Discovery to Disaster. *J Young Pharm* **2:**332-336.

Barre-Sinoussi F and Montagutelli X (2015) Animal models are essential to biological research: issues and perspectives. *Future Sci OA* **1:**FSO63.

Basit A, Neradugomma NK, Wolford C, Fan PW, Murray B, Takahashi RH, Khojasteh SC, Smith BJ, Heyward S, Totah RA, Kelly EJ, and Prasad B (2020) Characterization of Differential Tissue Abundance of Major Non-CYP Enzymes in Human. *Molecular pharmaceutics* **17:**4114-4124.

Basit A, Radi Z, Vaidya VS, Karasu M, and Prasad B (2019) Kidney Cortical Transporter Expression across Species Using Quantitative Proteomics. *Drug Metab Dispos* **47:**802-808.

Bhatt DK and Prasad B (2018) Critical Issues and Optimized Practices in Quantification of Protein Abundance Level to Determine Interindividual Variability in DMET Proteins by LC-MS/MS Proteomics. *Clin Pharmacol Ther* **103:**619-630.

Di L (2019) The Impact of Carboxylesterases in Drug Metabolism and Pharmacokinetics. *Curr Drug Metab* **20:**91-102.

Diamond S, Boer J, Maduskuie TP, Jr., Falahatpisheh N, Li Y, and Yeleswaram S (2010) Species-specific metabolism of SGX523 by aldehyde oxidase and the toxicological implications. *Drug Metab Dispos* **38:**1277-1285.

Diao X and Huestis MA (2019) New Synthetic Cannabinoids Metabolism and Strategies to Best Identify Optimal Marker Metabolites. *Front Chem* **7:**109.

Glaenzel U, Jin Y, Hansen R, Schroer K, Rahmanzadeh G, Pfaar U, Jaap van Lier J, Borell H, Meissner A, Camenisch G, and Zhao S (2020) Absorption, Distribution, Metabolism, and Excretion of Capmatinib (INC280) in Healthy Male Volunteers and In Vitro Aldehyde Oxidase Phenotyping of the Major Metabolite. *Drug Metab Dispos* **48:**873-885.

Hammer H, Schmidt F, Marx-Stoelting P, Potz O, and Braeuning A (2021) Cross-species analysis of hepatic cytochrome P450 and transport protein expression. *Arch Toxicol* **95:**117-133.

Hanioka N, Saito K, Isobe T, Ohkawara S, Jinno H, and Tanaka-Kagawa T (2021) Favipiravir biotransformation in liver cytosol: Species and sex differences in humans, monkeys, rats, and mice. *Biopharm Drug Dispos* **42:**218-225.

Lepper ER, Smith NF, Cox MC, Scripture CD, and Figg WD (2006) Thalidomide metabolism and hydrolysis: mechanisms and implications. *Curr Drug Metab* **7:**677-685.

Lolkema MP, Bohets HH, Arkenau HT, Lampo A, Barale E, de Jonge MJA, van Doorn L, Hellemans P, de Bono JS, and Eskens F (2015) The c-Met Tyrosine Kinase Inhibitor JNJ-38877605 Causes Renal Toxicity through Species-Specific Insoluble Metabolite Formation. *Clin Cancer Res* **21:**2297-2304.

Manevski N, King L, Pitt WR, Lecomte F, and Toselli F (2019) Metabolism by Aldehyde Oxidase: Drug Design and Complementary Approaches to Challenges in Drug Discovery. *J Med Chem* **62:**10955-10994.

Nau H (2001) Teratogenicity of isotretinoin revisited: species variation and the role of all-trans-retinoic acid. *J Am Acad Dermatol* **45:**S183-187.

Needs CJ and Brooks PM (1985) Antirheumatic medication in pregnancy. *Br J Rheumatol* **24:**282-290.

Parvez MM, Basit A, Jariwala PB, Gaborik Z, Kis E, Heyward S, Redinbo MR, and Prasad B (2021) Quantitative investigation of irinotecan metabolism, transport and gut microbiome activation. *Drug Metab Dispos*.

Prasad B, Bhatt DK, Johnson K, Chapa R, Chu X, Salphati L, Xiao G, Lee C, Hop C, Mathias A, Lai Y, Liao M, Humphreys WG, Kumer SC, and Unadkat JD (2018) Abundance of Phase 1 and 2 Drug-Metabolizing Enzymes in Alcoholic and Hepatitis C Cirrhotic Livers: A Quantitative Targeted Proteomics Study. *Drug Metab Dispos* **46:**943-952.

Semino-Mora C, Leon-Monzon M, and Dalakas MC (1997) Mitochondrial and cellular toxicity induced by fialuridine in human muscle in vitro. *Lab Invest* **76:**487-495.

Uehara S, Yoneda N, Higuchi Y, Yamazaki H, and Suemizu H (2021) Oxidative metabolism and pharmacokinetics of the EGFR inhibitor BIBX1382 in chimeric NOG-TKm30 mice transplanted with human hepatocytes. *Drug Metab Pharmacokinet* **41:**100419.

Wang L, Prasad B, Salphati L, Chu X, Gupta A, Hop CE, Evers R, and Unadkat JD (2015) Interspecies variability in expression of hepatobiliary transporters across human, dog, monkey, and rat as determined by quantitative proteomics. *Drug Metab Dispos* **43:**367-374.

Wang P, Jia Y, Wu R, Chen Z, and Yan R (2021) Human gut bacterial beta-glucuronidase inhibition: An emerging approach to manage medication therapy. *Biochem Pharmacol* **190:**114566.

Wang YQ, Shang XF, Wang L, Zhang P, Zou LW, Song YQ, Hao DC, Fang SQ, Ge GB, and Tang H (2020) Interspecies variation of clopidogrel hydrolysis in liver microsomes from various mammals. *Chem Biol Interact* **315:**108871.

Zou L, Stecula A, Gupta A, Prasad B, Chien HC, Yee SW, Wang L, Unadkat JD, Stahl SH, Fenner KS, and Giacomini KM (2018) Molecular Mechanisms for Species Differences in Organic Anion Transporter 1, OAT1: Implications for Renal Drug Toxicity. *Mol Pharmacol* **94:**689-699.

Footnotes

- This work was funded by Proteomics-based Research Initiative for Non-CYP Enzymes (PRINCE) consortium: Genentech Inc., Gilead Sciences Inc., and Merck & Co., Inc.
- The authors declare that they have no conflicts of interest with the contents of this article.

Legends for Figures

Figure 1. Protein sequence similarity (%) of various non-CYP enzymes between human and preclinical species. The nomenclature of AOX and UGTs is not consistent across species. i) Dogs do not express AOX1 and therefore AOX2 was quantified in dogs as it showed >60% sequence similarity with human AOX1. ii) Human UGT1A3 has the closest sequence similarity to UGT1A4 in cynomolgus monkey (93%). iii) Human UGT2B4 has closet sequence similarity to UGT2B19 or 2B30 in monkey (88%), UGT2B31 in dog (78%), UGT2B31 or 2B10 in rat (71%). iv) Human UGT2B7 has closest sequence similarity to UGT2B9 or UGT2B18 in cynomolgus monkey (90%), UGT2B31 in dog (75%) and UGT2B4 or 2B10 in mouse (70%). v) Human UGT2B15 has the closest sequence similarity to UGT2B20 in rhesus monkey (92%) and UGT2B31 in dog (76%). vi) Human UGT2B17 has closest sequence similarity to UGT1A4a in cynomolgus monkey (93%), UGT2B20 in rhesus monkey (90%), UGT2B31 in dog (78%), UGT2B1 in rat (71%), and UGT2B4 in mouse (71%). Details are provided in Supplementary Table S4.

Figure 2: Comparison of absolute abundance (pmol/mg S9 protein) of non-CYP enzyme in human and monkey across tissues. The data is presented for the proteins sharing conserved peptides between human and monkey.

Figure 3: Relative hepatic abundance (per mg of S9 protein) of non-CYP DMEs across species. X-axis represent the species (H = Human, C = Cynomolgus monkey, RH = Rhesus monkey, D = Beagle Dog, SD = Sprague Dawley Rat, WH = Wistar Han rat and M = CD1 mouse) and y-axis represent the relative protein abundance per mg protein. Table S5 contains absolute abundance data for proteins where the peptide calibrators are available.

Figure 4: Extrahepatic to hepatic ratio for non-CYP DMEs across species. **ND** = Not detected due to non-conserved isoform, **α** = Intestinal specific abundance

Figure 5: Factors affecting interspecies extrapolation of non-CYP drug metabolism

DMD Fast Forward. Published on December 30, 2021 as DOI: 10.1124/dmd.121.000774
This article has not been copyedited and formatted. The final version may differ from this version.

TABLES

Table 1: Characteristics and Source of Tissues from Preclinical Species

Species	Tissue	Donor (n)	Sex	Pooled/Individual	Source
CD1 mouse	liver	12	M	Pooled	BioIVT
	Kidney	12	M	Pooled	BioIVT
	Intestine	12	M	Pooled	BioIVT
	Heart	12	M	Pooled	BioIVT
SD Rat	liver	6	M	Pooled	BioIVT
	Kidney	6	M	Pooled	BioIVT
	Intestine	200	M	Pooled	SEKISUI XenoTech
	Heart	6	M	Pooled	BioIVT
WH Rat	liver	240	M	Pooled	SEKISUI XenoTech
	Kidney	6	M	Pooled	BioIVT
	Intestine	6	M	Pooled	BioIVT
	Heart	6	M	Pooled	BioIVT
Beagle Dog	Liver	3	2 M, 1 F	Individual	BioIVT
	Kidney	3	M	Individual	BioIVT
	Intestine	3	M	Individual	BioIVT
	Heart	3	M	Individual	BioIVT
Cynomolgus	Liver	4	M	Individual	BioIVT
	Kidney	3	M	Individual	BioIVT
	Intestine	4	M	Individual	BioIVT
	Heart	1	M	Individual	BioIVT
Rhesus	Liver	6	M	Pooled	SEKISUI XenoTech
	Intestine	7	M	Pooled	SEKISUI XenoTech
Human*	Liver	21	12 M, 9 F	Individual	University of Washington
	Kidney	22	13 M, 9 F	Individual	University of Washington
	Intestine	14	10 M, 4 F	Individual	BioIVT
	Heart	17	10 M, 7 F	Individual	University of Washington

*Previously analyzed human data were used to compare cross-species differences in DME abundance.

DMD Fast Forward. Published on December 30, 2021 as DOI: 10.1124/dmd.121.000774
This article has not been copyedited and formatted. The final version may differ from this version.

Table 2: Reported data on the localization of AOX isoforms in preclinical species and human

Protein	Tissue(s)				
	Mouse	**Rat**	**Dog**	**Monkey**	**Human**
AOX1	Liver, esophagus, lung, heart, Harderian gland, olfactory mucosa, skin, testis, brain, spinal cord, and eye	Liver, heart, lung, spleen, and kidney	NP	Liver, lung, kidney, lacrimal gland and olfactory mucosa	Liver, adipose tissue, lung, skeletal muscle, and pancreas
AOX2	Olfactory mucosa epithelium and skin	Unknown	Thyroid gland	Nasal mucosa	NP
AOX3	Liver	Unknown		NP	NP
AOX4	Harderian glands, sebaceous glands, epidermis, and testis	Harderian glands, sebaceous glands, epidermis, and testis	Nose, Mammary glands, skin, testis, brain	NP	NP

Unknown indicates that the protein is expressed, but the localization is not characterized. NP = Gene or protein not present

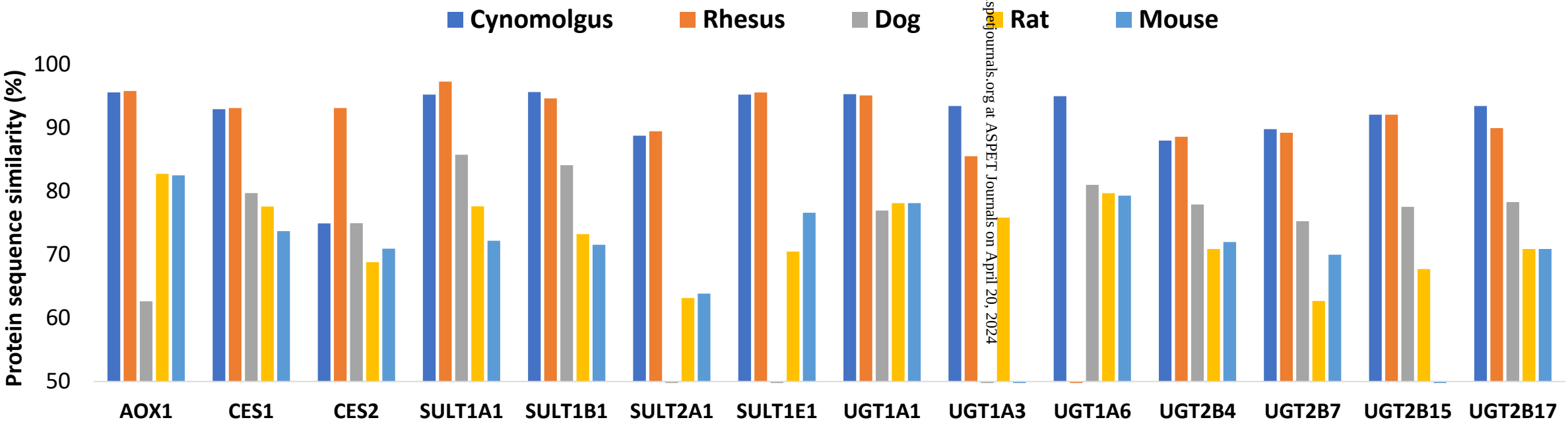

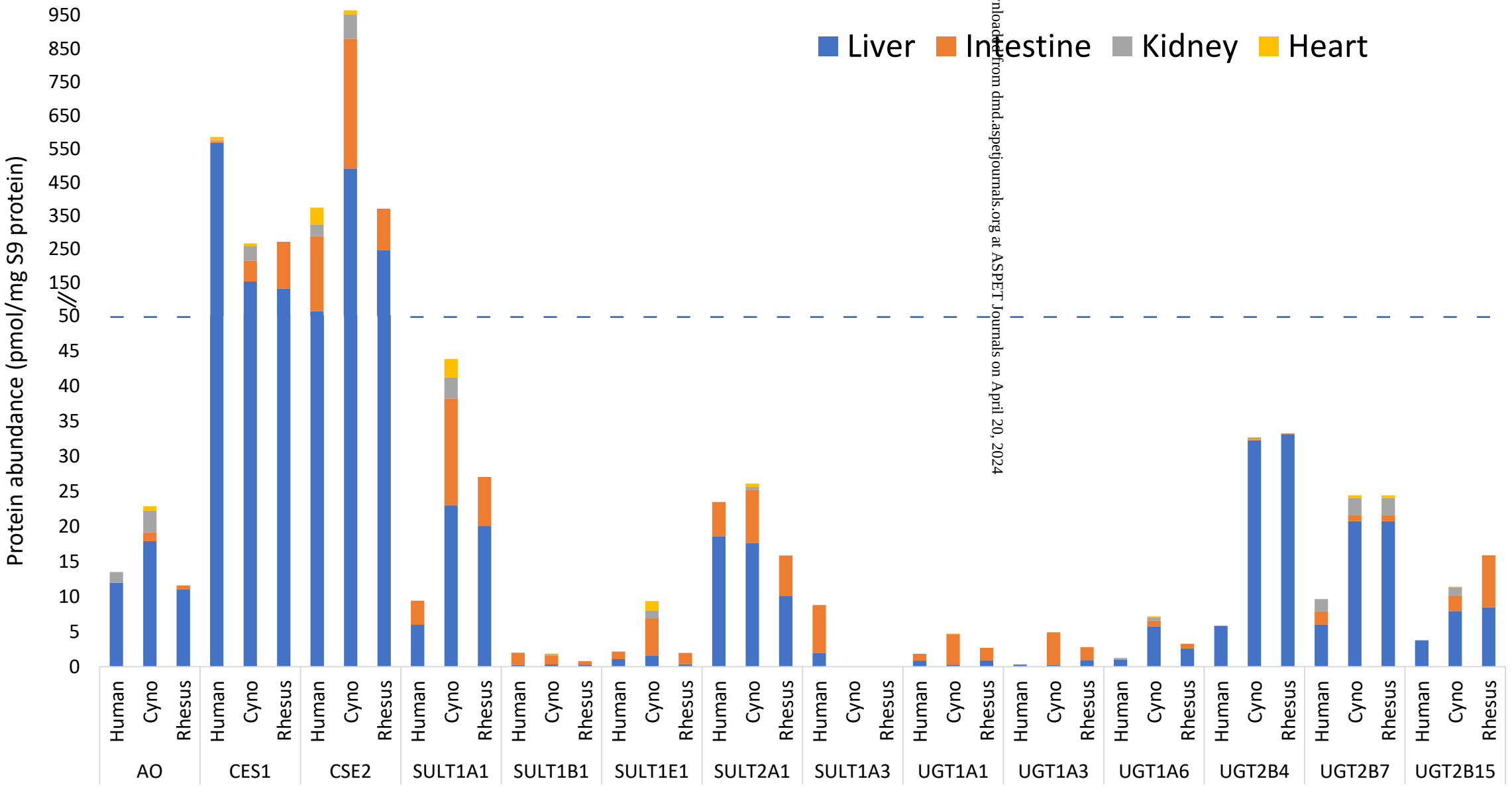

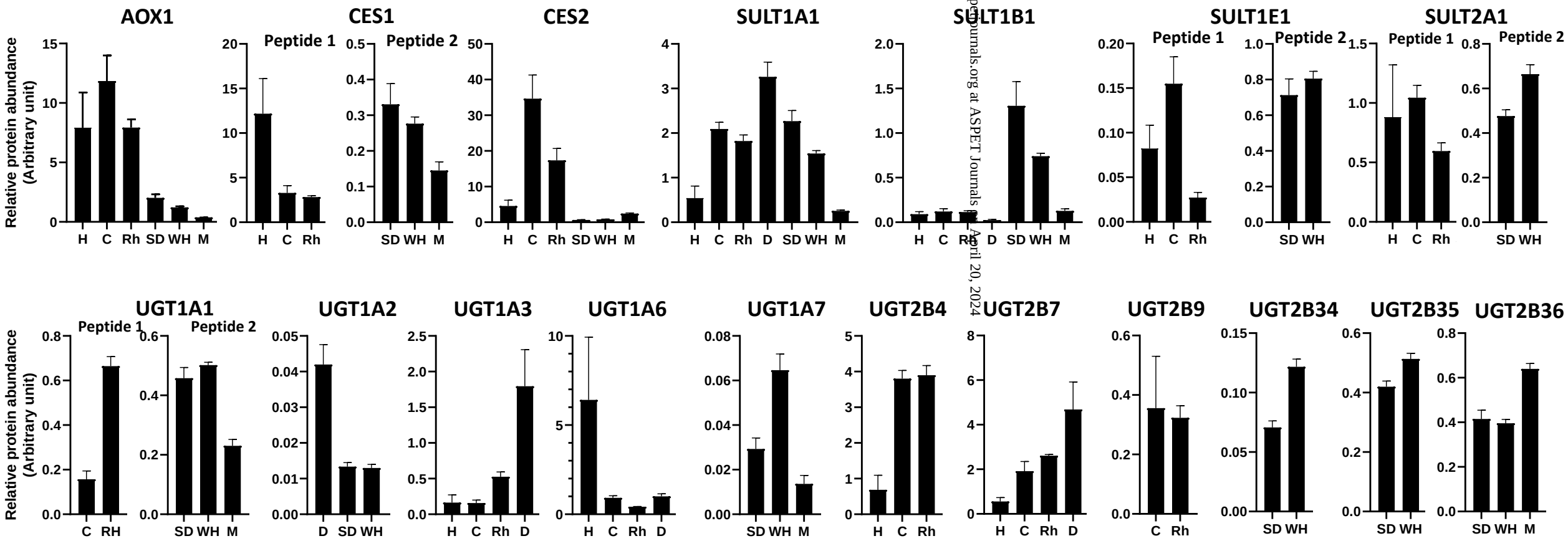

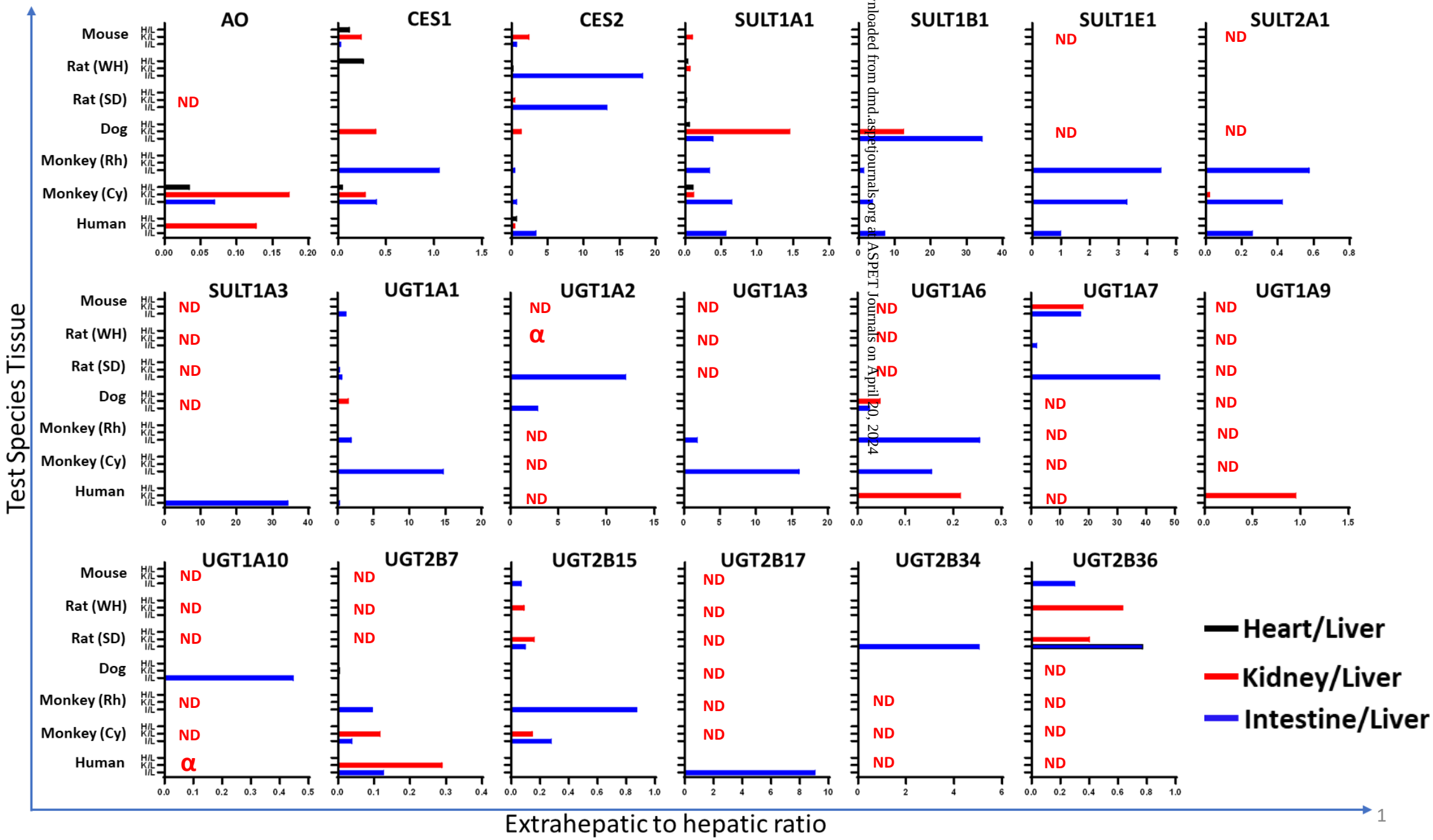

Interspecies protein abundance difference

Protein sequence homology

$$CL_{int} = \frac{Vmax}{Km+[S]} = \frac{[Abundance\ x\ Kcat]}{Km+[S]}$$

Tissue specific *fm*

Differential tissue abundance

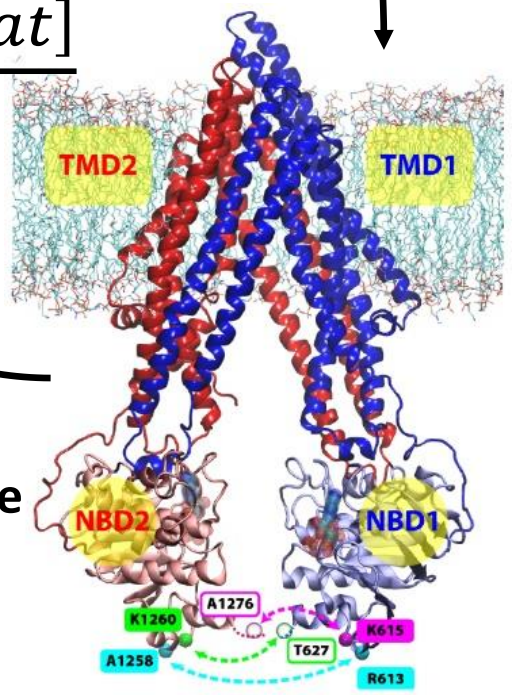

Active site

$$CL_{int,\,human}\ \alpha\ CL_{int,\,animal}\ x\ \frac{[Abundance_{human}]}{[Abundance_{animal}]}\ \text{x}\ \frac{[K_{m,animal}]}{[K_{m,human}]}$$

SUPPLEMENTARY INFORMATION

Comparison of tissue abundance of non-cytochrome P450 drug metabolizing enzymes by quantitative proteomics between humans and laboratory animal species

Abdul Basit[1], Peter W. Fan[2], S. Cyrus Khojasteh[3], Bernard P. Murray[4], Bill J. Smith[4], Scott Heyward[5], and Bhagwat Prasad[1]

[1]Department of Pharmaceutical Sciences, Washington State University, Spokane, WA 99202

[2]Department of Pharmacokinetics, Pharmacodynamics and Drug Metabolism Merck & Co., Inc. 33 Avenue Louis Pasteur Boston, MA 02115

[3]Department of Drug Metabolism and Pharmacokinetics, Genentech Inc., 1 DNA Way, MS 412a, South San Francisco, CA 94080

[4]Drug Metabolism and Pharmacokinetics Department, Gilead Sciences Inc., 324 Lakeside Drive, Foster City CA 94404

[5]BioIVT Inc., Baltimore, MD, 21227

***Corresponding author:** Bhagwat Prasad, Ph.D., Department of Pharmaceutical Sciences, Washington State University, Spokane, WA 99202, USA. Phone: +1-509-358-7739. Fax: +1 509-368-6561. Email: bhagwat.prasad@wsu.edu

Supplementary Table S1: Demographic information of human tissue donors

Organ	Total sample number	Subcellular fraction	Age (yr)	Gender/Ethnicity (number of samples)
Liver	21	S9	15- 64	M/C (10); M/AA (2); F/C (9)
Intestine	14	Microsomes	33- 67	M/C (8); F/C (1); M/AA (1); F/AA (2); M/H (1); F/H (1)
Kidney	22	S9	47- 76	M/C (11); M/H (2); F/C (9)
Heart	17	S9	65 - 78	M/HI (3); M/C (6); M/AA (1); F/HI (1); F/C (4); F/AA (2)
Lung	11	S9	2-66	M/C (4); F/C (2); M/AA (2); F/AA (1); M/H (2)

M=Male; F=Female. C=Caucasian; H= Hispanic; AA=African American.

Supplementary Table S2: Identification and detection of surrogate peptides for non-CYP DMEs. Green color indicates that surrogate or conserved peptide were available. Orange color indicates non-conserved peptides for which the matrix approach (PMID: 31123036) was used for extrapolations.

Protein	Peptides	Human	Monkey (Cynomolgus)	Monkey (Rhesus)	Dog	Rat (SD)	Rat (WH)	Mouse
AO	MIQVVSR							
	NLIQCWR							
	ELFLTFVTSSR							
CES1	TPEELQAER							
	TEDELLETSLK							
	EGYLQIGIPTQPAQK							
	FNSVPYIIGINK							
	EGYLQIGANTQAAQK							
CES2	WVQQNIAHFGGNPDR							
	LQFWTK							
	FFPAVVDGTFLPR							
	HATGNWGYLDQVAALR							
SULT1A1	THLPLSLLPQSLLDQK							
	ILEFLGR							
	VPFLEFK							
	THLPLALLPQTLLDQK							
SULT1B1	NYFTVAQNEK							
	THLPTDLLPK							
	THLPIDLLPK							
SULT1E1	NHFTVALNEK							
	NEDLINGIK							
	SFSEFVEK							
SULT2A1	LFSSHLPIQLFPK							
	TLEPEELNLILK							
	WIQSVTIWDR							
	NFLLLSYEELK							
SULT1A3	AHPEPGTWDSFLEK							
UGT1A1	DGAFYTLK							
	YLSIPTVFFLR							
	GVFENVPLLR							
	SVFDQDPFLLR							
	VVYSPYGSLATEILQK							
	EGSFYTLR							
	TAFNQDSFLLR							

UGT1A2	TATLIFQR GEDFFTLQTYAFPYTK YICHLSITPYESLASELLQR
UGT1A3	YLSIPTVFFLR ILLGQSYLVFER AAALIFQR
UGT1A6	DIVEVLSDR SFLTAPQTEYR GHDIVVLVPEVNLLLK SPNPVSYIPR
UGT1A7	FFIDSQWK YFSLPSVVFSR IFIDAQWK
UGT1A9	SFLTGSAR YFSLPSVIFAR
UGT1A10	TYSTSYTLEDQNR YFSLPSVVFTR
UGT2B4	ANVIASALAK FEVYPVSLTK
UGT2B7	TILDELIQR ANVIASALAQIPQK
UGT2B9	IEVYPTSLTK
UGT2B15	NYLEDSLLK SVINDPVYK TILEELVR FEVYPTSLTK SVINEPIYK SDLLNALEEVIDNPFYK
UGT2B17	FSVGYTVEK SVINDPIYK
UGT2B34	IPLVYSLR
UGT2B35	FSPGYTIEK
UGT2B36	IILDELK FSPGYYLEK TPATLGPNTR SDLLNALEEVIDNPFYK

Amino acid shown in blue color are showing subtle changes in the peptide sequence across species when the conserved peptides were not available, and the matrix approach was not applicable.

Supplementary Table S3: Multiple reaction monitoring (MRM) transitions and mass spectrometric parameters for peptides

Protein	Peptides	Label	Parent Ion (m/z)	Daughter Ion (m/z)	CV	CE
UGT1A1	DGAFYTLK	Light	457.73	671.38	35	16
			457.73	524.31	35	16
			457.73	244.09	35	16
		Heavy	461.74	679.39	35	16
			461.74	532.32	35	16
			461.74	244.09	35	16
	YLSIPTVFFLR	Light	678.39	879.51	35	24
			678.39	435.27	35	24
			678.39	277.15	35	24
			678.39	364.19	35	24
		Heavy	683.39	889.52	35	24
			683.39	445.28	35	24
			683.39	277.15	35	24
			683.39	364.19	35	24
	GVFENVPLLR	Light	572.33	840.49	35	20
			572.33	711.45	35	20
			572.33	498.34	35	20
		Heavy	577.33	850.50	35	20
			577.33	721.46	35	20
			577.33	508.35	35	20
	SVFDQDPFLLR	Light	668.85	1150.59	35	24
			668.85	1003.52	35	24
			668.85	760.43	35	24
			668.85	645.41	35	24
		Heavy	673.85	1160.59	35	24
			673.85	1013.52	35	24
			673.85	770.44	35	24
			673.85	655.41	35	24
	VVYSPYGSLATEILQK	Light	884.48	1319.72	35	32
			884.48	1059.60	35	32
			884.48	802.46	35	32
		Heavy	888.49	1327.73	35	32
			888.49	1067.61	35	32
			888.49	810.48	35	32
	EGSFYTLR	Light	486.74	699.38	35	17
			486.74	552.31	35	17
			486.74	389.25	35	17

			486.74	288.20	35	17
		Heavy	491.75	709.39	35	17
			491.75	562.32	35	17
			491.75	399.25	35	17
			491.75	298.21	35	17
	TAFNQDSFLLR	Light	656.34	992.51	35	23
			656.34	878.47	35	23
			656.34	750.41	35	23
		Heavy	661.34	1002.52	35	23
			661.34	888.48	35	23
			661.34	760.42	35	23
UGT1A2	TATLIFQR	Light	475.28	777.46	35	17
			475.28	563.33	35	17
			475.28	450.25	35	17
		Heavy	480.28	787.47	35	17
			480.28	573.34	35	17
			480.28	460.25	35	17
	GEDFFTLQTYAFPYTK	Light	478.74	508.31	35	17
			478.74	361.24	35	17
			478.74	187.07	35	17
		Heavy	482.75	516.32	35	17
			482.75	369.25	35	17
			482.75	187.07	35	17
UGT1A3	ILLGQSYLVFER	Light	719.41	913.48	35	26
			719.41	826.45	35	26
			719.41	451.23	35	26
		Heavy	724.41	923.49	35	26
			724.41	836.45	35	26
			724.41	461.24	35	26
	AAALIFQR	Light	445.27	563.33	35	15
			445.27	450.25	35	15
			445.27	214.12	35	15
		Heavy	450.27	573.34	35	15
			450.27	460.25	35	15
			450.27	214.12	35	15
UGT1A6	DIVEVLSDR	Light	523.28	817.44	35	18
			523.28	718.37	35	18
			523.28	589.33	35	18
			523.28	229.12	35	18
			523.28	229.12	35	18
		Heavy	528.28	827.45	35	18

			528.28	728.38	35	18
			528.28	599.34	35	18
			528.28	229.12	35	18
			528.28	229.12	35	18
	SFLTAPQTEYR	Light	656.83	965.47	35	23
			656.83	864.42	35	23
			656.83	793.38	35	23
		Heavy	661.83	975.48	35	23
			661.83	874.43	35	23
			661.83	803.39	35	23
	GHDIVVLVPEVNLLLK	Light	586.69	925.57	35	20
			586.69	621.34	35	20
			586.69	734.42	35	20
		Heavy	589.36	933.59	35	20
			589.36	621.34	35	20
			589.36	734.42	35	20
	SPNPVSYIPR	Light	565.30	945.52	35	20
			565.30	831.47	35	20
			565.30	635.35	35	20
			565.30	272.17	35	20
		Heavy	570.31	955.52	35	20
			570.31	841.48	35	20
			570.31	645.36	35	20
			570.31	282.18	35	20
UGT1A7	FFIDSQWK	Light	535.76	776.39	35	19
			535.76	663.30	35	19
			535.76	548.28	35	19
		Heavy	539.77	784.40	35	19
			539.77	671.32	35	19
			539.77	556.29	35	19
	YFSLPSVVFSR	Light	651.34	991.55	35	23
			651.34	904.52	35	23
			651.34	791.44	35	23
			651.34	508.28	35	23
		Heavy	656.35	1001.56	35	23
			656.35	914.53	35	23
			656.35	801.44	35	23
			656.35	518.29	35	23
	IFIDAQWK	Light	510.77	760.39	35	18
			510.77	647.31	35	18
			510.77	261.15	35	18

		Heavy	514.78	768.41	35	18
			514.78	655.32	35	18
			514.78	261.15	35	18
UGT1A9	SFLTGSAR	Light	419.72	604.34	35	14
			419.72	491.25	35	14
			419.72	390.20	35	14
			419.72	235.10	35	14
		Heavy	424.72	614.34	35	14
			424.72	501.26	35	14
			424.72	400.21	35	14
			424.72	235.10	35	14
	YFSLPSVIFAR	Light	650.35	989.57	35	23
			650.35	902.54	35	23
			650.35	789.46	35	23
			650.35	398.17	35	23
		Heavy	650.35	999.58	35	23
			650.35	912.55	35	23
			650.35	799.47	35	23
			650.35	398.17	35	23
UGT1A10	TYSTSYTLEDQNR	Light	789.36	875.42	35	28
			789.36	661.29	35	28
			789.36	265.12	35	28
		Heavy	794.36	885.43	35	28
			794.36	671.30	35	28
			794.36	265.12	35	28
	YFSLPSVVFTR	Light	658.36	1005.57	35	23
			658.36	805.46	35	23
		Heavy	663.36	1015.58	35	23
			663.36	815.46	35	23
UGT2B4	ANVIASALAK	Light	479.29	560.34	35	17
			479.29	186.09	35	17
			479.29	285.16	35	17
		Heavy	483.30	568.35	35	17
			483.30	186.09	35	17
			483.30	285.16	35	17
	FEVYPVSLTK	Light	591.82	906.52	35	21
			591.82	644.39	35	21
			591.82	277.11	35	21
		Heavy	595.83	914.54	35	21
			595.83	652.41	35	21
			595.83	277.11	35	21

UGT2B7	TILDELIQR	Light	550.82	886.49	35	19
			550.82	773.41	35	19
			550.82	658.38	35	19
		Heavy	555.82	896.50	35	19
			555.82	783.42	35	19
			555.82	668.39	35	19
	ANVIASALAQIPQK	Light	712.41	684.40	35	25
			712.41	372.22	35	25
			712.41	285.15	35	25
		Heavy	716.42	692.41	35	25
			716.42	380.23	35	25
			716.42	285.151	35	25
UGT2B9	IEVYPTSLTK	Light	575.82	908.51	35	20
			575.82	809.44	35	20
			575.82	646.38	35	20
		Heavy	579.83	916.52	35	20
			579.83	817.45	35	20
			579.83	654.39	35	20
UGT2B15	NYLEDSLLK	Light	547.79	817.47	35	19
			547.79	704.38	35	19
			547.79	278.11	35	19
		Heavy	551.80	825.48	35	19
			551.80	712.40	35	19
			551.80	278.11	35	19
	SVIN**D**P**V**YK	Light	517.78	848.45	35	18
			517.78	735.37	35	18
			517.78	187.11	35	18
		Heavy	521.79	856.47	35	18
			521.79	743.38	35	18
			521.79	187.11	35	18
	TILEELVR	Light	486.79	758.44	35	17
			486.79	645.36	35	17
			486.79	516.31	35	17
			486.79	215.14	35	17
		Heavy	491.79	768.45	35	17
			491.79	655.36	35	17
			491.79	526.32	35	17
			491.79	215.14	35	17
	FEVYPTSLTK	Light	592.81	908.51	35	21
			592.81	809.44	35	21
			592.81	646.38	35	21

			592.81	277.12	35	21
		Heavy	596.82	916.52	35	21
			596.82	817.45	35	21
			596.82	654.39	35	21
			596.82	277.12	35	21
	SVINEPIYK	Light	531.80	876.48	35	19
			531.80	763.40	35	19
			531.80	520.31	35	19
			531.80	187.11	35	19
		Heavy	535.80	884.50	35	19
			535.80	771.41	35	19
			535.80	528.33	35	19
			535.80	187.11	35	19
	SDLLNALEEVIDNPFYK	Light	660.67	896.45	35	22
			660.67	783.37	35	22
			660.67	668.34	35	22
		Heavy	663.34	904.47	35	22
			663.34	791.38	35	22
			663.34	676.35	35	22
UGT2B17	FSVGYTVEK	Light	515.27	882.46	35	18
			515.27	795.42	35	18
			515.27	696.36	35	18
			515.27	476.27	35	18
		Heavy	519.27	890.47	35	18
			519.27	803.44	35	18
			519.27	704.37	35	18
			519.27	484.29	35	18
	SVINDPIYK	Light	524.79	862.47	35	18
			524.79	749.38	35	18
			524.79	520.31	35	18
			524.79	187.11	35	18
		Heavy	528.79	870.48	35	18
			528.79	757.40	35	18
			528.79	528.33	35	18
			528.79	187.11	35	18
UGT2B34	IPLVYSLR	Light	480.79	847.50	35	17
			480.79	750.45	35	17
			480.79	637.36	35	17
			480.79	538.29	35	17
		Heavy	485.80	857.51	35	17
			485.80	760.45	35	17

			485.80	647.37	35	17
			485.80	548.30	35	17
UGT2B35	FSPGYTIEK	Light	521.26	894.45	35	18
			521.26	710.37	35	18
			521.26	653.35	35	18
		Heavy	525.27	902.47	35	18
			525.27	718.38	35	18
			525.27	661.36	35	18
UGT2B36	IILDELK	Light	422.26	730.43	35	15
			422.26	617.35	35	15
			422.26	260.19	35	15
			422.26	227.17	35	15
		Heavy	426.27	738.44	35	15
			426.27	625.36	35	15
			426.27	268.21	35	15
			426.27	227.17	35	15
	FSPGYYLEK	Light	552.27	869.44	35	19
			552.27	772.38	35	19
			552.27	235.10	35	19
		Heavy	556.28	877.45	35	19
			556.28	780.40	35	19
			556.28	235.10	35	19
	TPATLGPNTR	Light	514.28	829.45	35	18
			514.28	758.41	35	18
			514.28	657.36	35	18
			514.28	544.28	35	18
		Heavy	519.28	839.46	35	18
			519.28	768.42	35	18
			519.28	667.37	35	18
			519.28	554.29	35	18
	SDLLNALEEVIDNPFYK	Light	660.67	896.45	35	22
			660.67	783.37	35	22
			660.67	668.34	35	22
		Heavy	663.34	904.47	35	22
			663.34	791.38	35	22
			663.34	676.35	35	22
BSA	LVNELTEFAK	Light	582.32	951.48	35	20
			582.32	708.39	35	20
			582.32	595.31	35	20
		Heavy	586.33	959.49	35	20
			586.33	716.41	35	20

			586.33	603.32	35	20
	AEFVEVTK	Light	461.75	722.41	35	16
			461.75	575.34	35	16
			461.75	476.27	35	16
		Heavy	465.75	730.42	35	16
			465.75	583.35	35	16
			465.75	484.29	35	16
AO	MIQVVSR	Light	416.74	588.35	35	14
			416.74	460.29	35	14
			416.74	361.22	35	14
			416.74	262.15	35	14
		Heavy	421.74	598.35	35	14
			421.74	470.30	35	14
			421.74	371.23	35	14
			421.74	272.16	35	14
	NLIQCWR	Light	495.25	762.37	35	17
			495.25	649.29	35	17
			495.25	521.23	35	17
			495.25	361.20	35	17
		Heavy	500.26	772.38	35	17
			500.26	659.30	35	17
			500.26	531.24	35	17
			500.26	371.21	35	17
	ELFLTFVTSSR	Light	650.35	1170.65	35	23
			650.35	797.42	35	23
			650.35	549.30	35	23
			650.35	349.18	35	23
		Heavy	655.35	1180.66	35	23
			655.35	807.42	35	23
			655.35	559.31	35	23
			655.35	359.19	35	23
CES1	TPEELQAER	Light	536.77	874.43	35	19
			536.77	745.38	35	19
			536.77	616.34	35	19
			536.77	375.20	35	19
			536.77	175.12	35	19
		Heavy	541.77	884.43	35	19
			541.77	755.39	35	19
			541.77	626.35	35	19
			541.77	385.21	35	19
			541.77	185.13	35	19

	TEDELLETSLK	Light	639.33	1047.56	35	23
			639.33	690.40	35	23
			639.33	448.28	35	23
		Heavy	643.33	1055.57	35	23
			643.33	698.42	35	23
			643.33	456.29	35	23
	EGYLQIG**IP**TQ**P**AQK	Light	821.94	1052.61	35	29
			821.94	939.53	35	29
			821.94	769.42	35	29
			821.94	443.26	35	29
		Heavy	825.95	1060.62	35	29
			825.95	947.54	35	29
			825.95	777.43	35	29
			825.95	451.28	35	29
	FNSVPYIIGINK	Light	682.88	1103.65	35	24
			682.88	917.55	35	24
			682.88	544.35	35	24
			682.88	431.26	35	24
			682.88	261.16	35	24
		Heavy	686.89	1111.66	35	24
			686.89	925.56	35	24
			686.89	552.36	35	24
			686.89	439.28	35	24
			686.89	269.17	35	24
	EGYLQIG**AN**TQ**A**AQK	Light	796.41	888.45	35	28
			796.41	417.25	35	28
			796.41	350.13	35	28
		Heavy	800.41	896.47	35	28
			800.41	425.26	35	28
			800.41	350.13	35	28
CES2	WVQQNIAHFGGNPDR	Light	580.29	970.45	35	20
			580.29	899.41	35	20
			580.29	615.28	35	20
		Heavy	583.62	980.46	35	20
			583.62	909.42	35	20
			583.62	625.29	35	20
	LQFWTK	Light	411.73	709.37	35	14
			411.73	581.31	35	14
			411.73	434.24	35	14
			411.73	248.16	35	14
		Heavy	415.74	717.38	35	14

			415.74	589.32	35	14
			415.74	442.25	35	14
			415.74	256.17	35	14
	FFPAVVDGTFLPR	Light	733.40	1171.65	35	26
			733.40	1003.56	35	26
			733.40	904.49	35	26
			733.40	805.42	35	26
			733.40	690.39	35	26
		Heavy	738.40	1181.66	35	26
			738.40	1013.57	35	26
			738.40	914.50	35	26
			738.40	815.43	35	26
			738.40	700.40	35	26
	HATGNWGYLDQVAALR	Light	591.30	772.43	35	20
			591.30	657.40	35	20
			591.30	529.35	35	20
			591.30	430.28	35	20
		Heavy	594.64	782.44	35	20
			594.64	667.41	35	20
			594.64	539.35	35	20
			594.64	440.29	35	20
SULT1A1	THLPL**S**LLPQ**S**LLDQK	Light	601.68	831.46	35	20
			601.68	616.37	35	20
			601.68	503.28	35	20
			601.68	390.20	35	20
			601.68	275.17	35	20
		Heavy	604.36	839.47	35	20
			604.36	624.38	35	20
			604.36	511.30	35	20
			604.36	398.21	35	20
			604.36	283.19	35	20
	ILEFLGR	Light	424.26	734.42	35	15
			424.26	621.34	35	15
			424.26	492.29	35	15
			424.26	345.22	35	15
			424.26	232.14	35	15
		Heavy	429.26	744.43	35	15
			429.26	631.34	35	15
			429.26	502.30	35	15
			429.26	355.23	35	15
			429.26	242.15	35	15

	VPFLEFK	Light	440.25	780.43	35	15
			440.25	683.38	35	15
			440.25	536.31	35	15
			440.25	294.18	35	15
		Heavy	444.26	788.44	35	15
			444.26	691.39	35	15
			444.26	544.32	35	15
			444.26	302.20	35	15
	THLPLALLPQTLLDQK	Light	601.02	942.53	35	20
			601.02	717.41	35	20
			601.02	390.20	35	20
			601.02	275.17	35	20
		Heavy	603.70	950.54	35	20
			603.70	725.43	35	20
			603.70	398.21	35	20
			603.70	283.19	35	20
SULT1B1	NYFTVAQNEK	Light	607.30	936.48	35	21
			607.30	789.41	35	21
			607.30	278.11	35	21
		Heavy	611.30	944.49	35	21
			611.30	797.42	35	21
			611.30	278.11	35	21
	THLPTDLLPK	Light	378.89	357.25	35	12
			378.89	244.17	35	12
			378.89	352.20	35	12
		Heavy	381.56	365.26	35	12
			381.56	252.18	35	12
			381.56	352.20	35	12
	THLPIDLLPK	Light	573.85	585.36	35	20
			573.85	470.33	35	20
			573.85	357.25	35	20
			573.85	244.17	35	20
		Heavy	577.85	593.37	35	20
			577.85	478.35	35	20
			577.85	365.26	35	20
			577.85	252.18	35	20
SULT2A1	LFSSHLPIQLFPK	Light	763.94	955.60	35	27
			763.94	842.51	35	27
			763.94	633.86	35	27
		Heavy	767.95	963.61	35	27
			767.95	850.53	35	27

			767.95	637.87	35	27
	TLEPEELNLILK	Light	706.41	1068.63	35	25
			706.41	600.41	35	25
			706.41	486.36	35	25
			706.41	344.18	35	25
		Heavy	710.41	1076.64	35	25
			710.41	608.42	35	25
			710.41	494.38	35	25
			710.41	344.18	35	25
	WIQSVTIWDR	Light	652.34	1004.52	35	23
			652.34	876.46	35	23
			652.34	789.43	35	23
			652.34	690.36	35	23
			652.34	589.31	35	23
		Heavy	657.35	1014.52	35	23
			657.35	886.47	35	23
			657.35	799.43	35	23
			657.35	700.37	35	23
			657.35	599.32	35	23
	NFLLLSYEELK	Light	684.87	994.55	35	24
			684.87	881.46	35	24
			684.87	768.38	35	24
			684.87	681.35	35	24
		Heavy	688.88	1002.56	35	24
			688.88	889.48	35	24
			688.88	776.39	35	24
			688.88	689.36	35	24
SULT1A3	AHPEPGTWDSFLEK	Light	538.59	738.37	35	18
			538.59	623.34	35	18
			538.59	209.10	35	18
		Heavy	541.26	746.38	35	18
			541.26	631.35	35	18
			541.26	209.10	35	18
SULT1E1	NHFTVALNEK	Light	391.54	574.32	35	13
			391.54	503.28	35	13
			391.54	500.23	35	13
		Heavy	394.21	582.33	35	13
			394.21	511.30	35	13
			394.21	500.23	35	13
	NEDLINGIK	Light	508.27	772.46	35	18
			508.27	657.43	35	18

			508.27	544.35	35	18
			508.27	431.26	35	18
			508.27	317.22	35	18
		Heavy	512.28	780.47	35	18
			512.28	665.44	35	18
			512.28	552.36	35	18
			512.28	439.28	35	18
			512.28	325.23	35	18
	SFSEFVEK	Light	486.74	738.37	35	17
			486.74	651.33	35	17
			486.74	522.29	35	17
			486.74	375.22	35	17
		Heavy	490.74	746.38	35	17
			490.74	659.35	35	17
			490.74	530.31	35	17
			490.74	383.24	35	17

Amino acid shown in blue color are showing subtle changes in the peptide sequence across species when the conserved peptides were not available, and the matrix approach was not applicable.

Supplementary Table 4: Protein sequence similarity (%) of various non-CYP enzymes between human and preclinical species.

Enzyme	Cynomolgus	Rhesus	Dog	Rat	Mouse
AOX1	95.59	95.82	62.65 (AOX2)*	82.74	82.51
CES1	92.95	93.13	79.72	77.60	73.72
CES2	74.93	93.13	74.96	68.81	70.95
SULT1A1	95.25	97.29	85.76	77.63	72.20
SULT1B1	95.65	94.65	84.12	73.24	71.57
SULT2A1	88.77	89.47	NA	63.16	63.86
SULT1E1	95.24	95.58	NA	70.49	76.61
UGT1A1	95.31	95.12	76.96	78.131	78.13
UGT1A3	93.45 (1A4)	85.53 (1A3 like)	NA	75.843	NA
UGT1A6	95	NA	81.02	79.699	79.32
UGT2B4	88 (2B19 or 2B30)*	88.6 (2B19 or 2B30) *	77.92 (2B31) *	70.89 (2B31, 2B10) *	72
UGT2B7	89.79 (2B9, 2B18)	89.225	75.28 (2B31) *	62.7	70 (2B4, 2B10) *
UGT2B15	92.08	92.08 (2B20) *	77.55 (2B31) *	67.73	NA
UGT2B17	93.45 (1A4a) *	89.96 (2B20) *	78.3 (2B31*)	70.89 (2B1) *	70.89 (2B4) *

Asterisk (*) Indicates the closest sequence similarity with human isoforms.

Supplementary Table S5: Absolute and relative quantification of non-CYP drug metabolizing enzymes in different tissues across preclinical species and human. Values highlighted in green indicate absolute quantification (pmol/mg S9 protein) using surrogate peptides. Values highlighted in orange or blue indicate the relative quantification. The relative values can be compared across preclinical species if they are shown in the same color. The protein abundance is presented as mean ± standard deviation.

Protein	Species	Liver	Intestine	Kidney	Heart
AO	Human	11.96 ± 4.46	BLQ	1.53 ± 0.79	BLQ
	Cynomolgus	17.87 ± 3.25	1.25 ± 0.19	3.11 ± 0.56	BLQ
	Rhesus	11.04 ± 1.04	0.55 ± 0.17	ND	ND
	Dog	BLQ	BLQ	BLQ	BLQ
	SD rat	3.05 ± 0.45	0.34 ± 0.02	0.2 ± 0.05	0.09 ± 0.01
	WH Rat	1.85 ± 0.13	0.41 ± 0.08	0.23 ± 0.02	0.28 ± 0.07
	Mouse	0.58 ± 0.04	0.02 ± 0.01	0.04 ± 0.02	0.08 ± 0.04
CES1	Human	569.06 ± 183.14	3.5 ± 4.58	3.65 ± 3.45	3.65 ± 3.45
	Cynomolgus	153.55 ± 38.03	62.37 ± 15.39	44.14 ± 17.91	BLQ
	Rhesus	132.13 ± 6.7	140.15 ± 39.89	ND	ND
	Dog	120.39 ± 20.15	2.11 ± 0.32	47.96 ± 16.49	0.24 ± 0.12
	SD rat	15.44 ± 2.7	2.06 ± 0.36	0.65 ± 0.02	1.58 ± 0.27
	WH Rat	12.91 ± 0.88	5.12 ± 0.5	0.73 ± 0.33	3.48 ± 0.78
	Mouse	17.83 ± 1.1	0.62 ± 0.07	1.35 ± 0.2	2.55 ± 0.12
CES2	Human	64.85 ± 22.86	224.34 ± 253.19	35.1 ± 18.76	50.36 ± 13.92
	Cynomolgus	491.7 ± 94.5	388.09 ± 129.31	72.49 ± 38.33	BLQ
	Rhesus	246.52 ± 47.13	124.76 ± 22.1	ND	ND
	Dog	9.84 ± 3.96	0.5 ± 0.11	13.71 ± 3.05	0.51 ± 0.16
	SD rat	9.26 ± 1.23	123.34 ± 27.67	5.13 ± 1.05	2.42 ± 0.65
	WH Rat	11.73 ± 1.28	214.33 ± 47.74	3.78 ± 2.37	6.83 ± 1.54
	Mouse	34.59 ± 2.29	26.43 ± 3.96	85.8 ± 29.67	2.77 ± 0.29
SULT1A1	Human	5.97 ± 2.95	3.44 ± 0.03	BLQ	BLQ
	Cynomolgus	23.02 ± 1.65	15.18 ± 3.71	2.98 ± 1.31	BLQ
	Rhesus	20.04 ± 1.52	6.99 ± 1.71	ND	ND
	Dog	35.91 ± 3.64	14.14 ± 3.72	52.57 ± 36.77	2.34 ± 0.23
	SD rat	24.96 ± 2.6	0.22 ± 0.05	0.73 ± 0.09	0.24 ± 0.04
	WH Rat	16.98 ± 0.35	0.12 ± 0.72	1.26 ± 0.38	0.81 ± 1.01
	Mouse	2.81 ± 0.23	0.02 ± 0.01	0.3 ± 0.08	0.25 ± 0.01
SULT1B1	Human	0.24 ± 0.07	1.75 ± 0.05	BLQ	BLQ
	Cynomolgus	0.31 ± 0.09	1.26 ± 0.16	0.16 ± 0.04	BLQ
	Rhesus	0.3 ± 0.04	0.49 ± 0.14	ND	ND
	Dog	0.06 ± 0.02	2.09 ± 0.32	0.77 ± 0.43	0 ± 0.02
	SD rat	3.38 ± 0.7	0.63 ± 0.1	0.97 ± 0.2	0.68 ± 0.23
	WH Rat	1.92 ± 0.08	0.56 ± 0.17	1.2 ± 0.09	1.24 ± 0.24

	Mouse	0.33 ± 0.06	0.04 ± 0.02	0.45 ± 0.21	0.75 ± 0.17
SULT1E1	Human	1.07 ± 0.34	1.09 ± 0.05	BLQ	BLQ
	Cynomolgus	1.61 ± 0.89	5.3 ± 1.19	1.05 ± 0.1	BLQ
	Rhesus	0.36 ± 0.08	1.6 ± 0.34	ND	ND
	Dog	NA	NA	NA	NA
	SD rat	9.3 ± 1.18	0.1 ± 0.02	0.2 ± 0.04	0.27 ± 0.08
	WH Rat	10.5 ± 0.54	0.3 ± 0.04	0.15 ± 0.03	0.48 ± 0.05
	Mouse	NA	NA	NA	NA
SULT2A1	Human	18.59 ± 9.31	4.88 ± 0.18	BLQ	BLQ
	Cynomolgus	17.64 ± 1.74	7.57 ± 3.1	0.41 ± 0.15	BLQ
	Rhesus	10.05 ± 1.17	5.79 ± 1.45	ND	ND
	Dog	NA	NA	NA	NA
	SD rat	8.05 ± 0.47	1.78 ± 1.36	0.56 ± 0.29	0.26 ± 0.03
	WH Rat	11.22 ± 1.1	2.4 ± 0.07	0.89 ± 0.09	1.17 ± 0.14
	Mouse	NA	NA	NA	NA
SULT1A3	Human	*0.198 ± 0.019*	6.80 ± 0.52	BLQ	BLQ
	Cynomolgus	NA	NA	NA	NA
	Rhesus	NA	NA	NA	NA
	Dog	NA	NA	NA	NA
	SD rat	NA	NA	NA	NA
	WH Rat	NA	NA	NA	NA
	Mouse	NA	NA	NA	NA
UGT1A1	Human	0.87 ± 0.59	0.97 ± 0.77	BLQ	BLQ
	Cynomolgus	0.29 ± 0.07	4.32 ± 2.3	0.07 ± 0.01	BLQ
	Rhesus	0.91 ± 0.11	1.78 ± 0.31	ND	ND
	Dog	0.31 ± 0.04	0.03 ± 0.01	0.49 ± 0.37	0 ± 0
	SD rat	0.85 ± 0.07	0.56 ± 0.03	0.31 ± 0.03	0.01 ± 0
	WH Rat	0.93 ± 0.02	0.13 ± 0.09	0.18 ± 0.01	0.02 ± 0.01
	Mouse	0.43 ± 0.04	0.55 ± 0.64	0.03 ± 0.01	0.02 ± 0
UGT1A3	Human	0.3 ± 0.19	0.03 ± 0.04	BLQ	BLQ
	Cynomolgus	0.29 ± 0.08	4.59 ± 2.48	0.04 ± 0.02	BLQ
	Rhesus	0.95 ± 0.12	1.84 ± 0.34	ND	ND
	Dog	3.25 ± 0.93	0.1 ± 0.02	0.16 ± 0.08	0.11 ± 0.06
	SD rat	NA	NA	NA	NA
	WH Rat	NA	NA	NA	NA
	Mouse	NA	NA	NA	NA
UGT1A4	Human	3.95 ± 2.52	BLQ	BLQ	BLQ
	Cynomolgus	NA	NA	NA	NA
	Rhesus	NA	NA	NA	NA
	Dog	NA	NA	NA	NA
	SD rat	NA	NA	NA	NA

	WH Rat	NA	NA	NA	NA
	Mouse	NA	NA	NA	NA
UGT1A6	Human	1.02 ± 0.5	BLQ	0.22 ± 0.29	BLQ
	Cynomolgus	5.7 ± 0.72	0.88 ± 0.31	0.41 ± 0.07	BLQ
	Rhesus	2.6 ± 0.09	0.66 ± 0.19	ND	ND
	Dog	6.2 ± 0.84	0.17 ± 0.05	0.3 ± 0.05	0.14 ± 0
	SD rat	NA	NA	NA	NA
	WH Rat	NA	NA	NA	NA
	Mouse	NA	NA	NA	NA
UGT1A9	Human	1.43 ± 0.44	BLQ	1.37 ± 0.92	BLQ
	Cynomolgus	NA	NA	NA	NA
	Rhesus	NA	NA	NA	NA
	Dog	NA	NA	NA	NA
	SD rat	NA	NA	NA	NA
	WH Rat	NA	NA	NA	NA
	Mouse	12.63 ± 1.08	0.34 ± 0.09	0.21 ± 0.06	0.18 ± 0.04
UGT1A10	Human	BLQ	4.35 ± 1.68	BLQ	BLQ
	Cynomolgus	NA	NA	NA	NA
	Rhesus	NA	NA	NA	NA
	Dog	14.52 ± 3.89	6.51 ± 1.46	3.14 ± 0.68	1.56 ± 0.32
	SD rat	NA	NA	NA	NA
	WH Rat	NA	NA	NA	NA
	Mouse	NA	NA	NA	NA
UGT2B4	Human	5.83 ± 3.46	BLQ	BLQ	BLQ
	Cynomolgus	32.25 ± 1.95	0.12 ± 0.08	0.23 ± 0.12	BLQ
	Rhesus	33.07 ± 2.31	0.17 ± 0.07	ND	ND
	Dog	NA	NA	NA	NA
	SD rat	NA	NA	NA	NA
	WH Rat	NA	NA	NA	NA
	Mouse	NA	NA	NA	NA
UGT2B7	Human	6.01 ± 1.9	1.88 ± 1.47	1.74 ± 1.17	BLQ
	Cynomolgus	20.73 ± 4.7	0.84 ± 0.46	2.47 ± 0.67	BLQ
	Rhesus	28.24 ± 0.64	2.73 ± 0.43	ND	ND
	Dog	50.74 ± 13.32	0.27 ± 0.02	0.3 ± 0.24	0.25 ± 0.04
	SD rat	NA	NA	NA	NA
	WH Rat	NA	NA	NA	NA
	Mouse	NA	NA	NA	NA
UGT2B15	Human	3.76 ± 1.56	BLQ	BLQ	BLQ
	Cynomolgus	7.93 ± 0.23	2.23 ± 1.31	1.17 ± 0.21	BLQ
	Rhesus	8.46 ± 0.81	7.41 ± 1.81	ND	ND
	Dog	NA	NA	NA	NA

	SD rat	4.26 ± 0.23	0.42 ± 0.07	0.69 ± 0.02	0.14 ± 0.03
	WH Rat	5.55 ± 0.09	1.44 ± 0.2	0.5 ± 0.06	0.17 ± 0.09
	Mouse	2.63 ± 0.15	0.19 ± 0.04	0.15 ± 0.06	0.16 ± 0.08
UGT2B17	Human	0.21 ± 0.26	1.31 ± 0.72	BLQ	BLQ
	Cynomolgus	NA	NA	NA	NA
	Rhesus	NA	NA	NA	NA
	Dog	NA	NA	NA	NA
	SD rat	NA	NA	NA	NA
	WH Rat	NA	NA	NA	NA
	Mouse	NA	NA	NA	NA

Supplementary Figure S1: Peptide selection strategy